



Published in final edited form as:

Acc Chem Res. 2013 March 19; 46(3): 632–641. doi:10.1021/ar300032q.

Custom-designed nanomaterial libraries for testing metal oxide toxicity

Suman Pokhrel[§], André E. Nel^ϕ, and Lutz Mädler^{§,*}

[§]Foundation Institute of Materials Science (IWT), Department of Production Engineering, University of Bremen, Germany

^ϕDepartment of Medicine-Division and California NanoSystems Institute at University of California, Los Angeles, California, USA

Conspectus

Advances in aerosol technology over the past 10 years have provided methods that enable the generation and design of ultrafine nanoscale materials for different applications. The particles are produced combusting a precursor solution and its chemical reaction in the in the gas phase. Flame spray pyrolysis (FSP) is a highly versatile technique for single step and scalable synthesis of nanoscale materials. New innovations in particle synthesis using FSP technology and its precursor chemistry have enabled flexible dry synthesis of loosely-agglomerated highly crystalline ultrafine powders (porosity ~90%) of binary, ternary and mixed binary or ternary oxides. The flame spray pyrolysis lies at the intersection of combustion science, aerosols technology and materials chemistry. The interdisciplinary research is not only inevitable but is becoming increasingly crucial in the design of nanoparticles (NPs) made in the gas phase. The increasing demand especially in the bio-applications for particles with specific material composition, high purity and crystallinity can be often fulfilled with the fast, single step FSP technique.

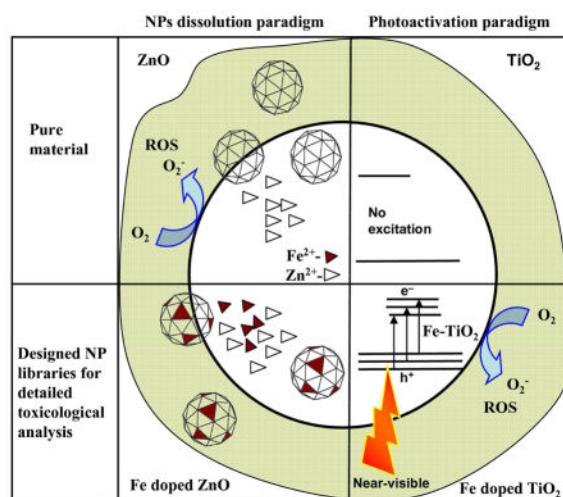
In this accounts we describe a strategy to design potential nanoparticles libraries (Pure or Fe doped ZnO or TiO₂) using versatile flame spray pyrolysis (FSP) and a strategy to use these libraries for testing different hypothesis related to toxicity paradigms. The innovation lies in the overall integration of the knowledge we developed in the last 5 years in (1) synthesizing hypothesis specific nanomaterials (2) demonstrating the electronic properties which are directly related to the material toxicity and (3) understanding the reaction mechanism involved during the toxicity testing (4) understanding hazardous nanomaterial properties that are essential for safe-design extracted from in-vitro to in vivo testing in different terrestrial and marine organisms. On the basis of these acquired knowledge, we further describe how the dissolved metal ion (Zn²⁺ in the present case) can effectively bind with different cell constituents. The Fe-S protein clusters have been chosen as a model example to demonstrate the complex chemical reactions that take place after the ionic migration into the cells.

As a second example, TiO₂ is an active material in the UV range and exhibits photocatalytic behaviour. The induction of electron-hole (e⁻/h⁺) pairs followed by free radical production

*Corresponding Author: Prof. Dr.-Ing. Lutz Mädler, IWT, Foundation Institute of Material Science, University of Bremen, 28359, Bremen, Germany, lmaedler@iwt.uni-bremen.de, Phone: 00-49-(0)421-218-51200, Fax: 00-49-(0)421-218-51211.

is a major conceptual paradigm for biological injury. We show that through decreasing the bandgap energy, the phototoxicity increases in the presence of near-visible light. The mechanism of electron transfer both in the biotic and abiotic system during light exposure is presented in detail. Here we show that FSP is again a versatile technique for efficiently designing a homologous library (parent oxide doped with different amount of dopant) and investigating their different properties.

Finally, we describe the future outlook and the state of the art of a new innovative two flame system. Double flame reactor enables control over independent flame, nozzle distances and flame angles for efficient mixing of the particle streams. In addition, different compositions, size and multicomponent mixing (grain-grain hetero-junction) during the reaction process can also be efficiently achieved.



Introduction

Many industrial sectors such as catalyst manufacturing, composite materials or passive electronic components include nanoparticles (NPs) in their processes. The market for nanotechnology based electronic components, and pharmaceuticals were \$147 billion in 2007 and are expected to reach \$2.5 trillion by 2015.^{1,2} Over the last decade, newly developed NPs have been found to exhibit fascinating properties.³ The development in NP production especially their specific design was mostly realized during the last twenty years. Initially, wet chemical routes were used for the preparation of oxide materials.^{4,5} Adapted from manufacturing of carbon black, the almost 70 years old industrial aerosol flame process was always a part of alternative methods for NP production. This dry synthetic method has advantages such as high purity and continuous production at high rates but was limited for a long time to simple metal oxides such as TiO_2 , Al_2O_3 and SiO_2 . Flame spray pyrolysis (FSP) was developed in the last decade and has developed into a very versatile technique in this family.⁶ The spectrum of NPs that can be produced is greatly enhanced with the FSP process that relies on the direct introduction of a liquid precursor into the flame producing highly dispersed, ultra-fine and single crystalline NPs.⁷ Due to enormously broad range of precursors available, FSP is one of the most promising single-step techniques for

the synthesis of a large class of binary, mixed binary, ternary and mixed ternary metal oxide NPs.⁶ This method overcomes the difficulty of bulk production and the complex chemical reactions involved. For example, synthesizing mixed oxide catalysts using precipitation method often involves the change of pH. However, the required pH can be very different for different oxide materials (e.g. Al₂O₃ and MgO) leading to a process with multiple precipitation steps. With the FSP method, however, complex mixtures are possible in a single step. Furthermore, this approach enables efficient *in-situ* manufacturing of NP layers and their patterning on different substrates.⁸ The state-of-the-art for designing homologous NP libraries (parent oxide doped with different amount of dopant) using versatile FSP technique is described in the supporting information.

Due to the small size of the NPs compared to their bulk counterparts, they have large number of surface atoms and therefore offer increased reactivity that enhance electron transfer, efficiently bind molecular species and easily translocate cell membranes when they are exposed to humans and the environment.⁹ In accordance to their attractive properties, NPs are utilized in advanced applications such as drug and gene delivery, biosensing, virus inhibition, and protein immobilization.¹⁰ These extraordinary properties, however, can in most cases not be deactivated at will. They are therefore omnipresent until the properties change due to environmental factors that can, for example lead to agglomeration. The increased use of nanoscale material might lead to increased likelihood of environmental and human exposure and has already raised concerns about their short and long-term toxicological and ecological effects.¹¹ Therefore, screening NPs toxicity for environmental implication becomes an important tool to predict possible biological injuries.¹² High content screening (search for chemical entities modulating important processes that can be imaged in biologically relevant cellular systems) permits parallel measurements of multiple parameters characterizing the cellular phenotype.¹³ Such considerations are being set in place before the commercial production of new nanoscale materials, exposure potential at work places, handling by the consumer and their final disposal.¹⁴

Custom designing ZnO or TiO₂ NP libraries using flame spray pyrolysis (FSP)

The current research activities on flame aerosol synthesis aim at developing cost-efficient routes to new and functional multicomponent and metastable NPs with the increased understanding of the chemical and physical principles underlying this process. In the flame environment, reactions and particle growth take place within milliseconds at high temperatures and the ability to rapidly quench these NP provide possibilities for doping metal oxides beyond their solubility limit and for creating metastable high temperature phases.⁸ Flame spray pyrolysis (FSP) is an attractive method (Figure S1 supplementary section) for NP production as it enables the use of wide range of precursors for different metal oxides. Particles can be re-engineered efficiently because each precursor droplet contains the same content of metals as desired in the product. In flame aerosol reactors, the energy of the flame generates the conditions for the NP growth, crystallization and morphological structure. The particles are formed in the gas phase through nucleation, surface growth, coagulation and coalescence^{15,16} in the flame environment during combustion of the dispersed droplets. The nanoparticle aerosol is collected after the particles are quenched to room temperature.¹⁷

In this accounts we focus on the designing combinatorial NP library (pure or Fe doped ZnO/TiO₂) and their high content screening process.¹² The choice of these materials to develop and evaluate the screening process was based on the demonstration of their differential toxic effects in a series of cellular assays.¹⁸ The cytotoxic and pro-inflammatory effects of ZnO particles are related to particle dissolution intra- and extracellularly.¹⁸ Particle generated ROS leads to a range of biological responses depending on the relative abundance of ROS and the type of cellular pathways that are induced through oxidative stress.¹¹ According to the hierarchical oxidative stress (OS), the lower OS includes activation of the antioxidant response element in the promoters of phase II genes by the transcription factors [Figure 1(e)–(g)] leading to the expression of cytoprotective enzymes.¹⁸ Only ZnO could generate a robust HO-1 message and protein expression in RAW 264.7 cells. The time dependent *in vivo* results show that (LDH) release, PMN cell count and albumin level decreased with Fe content [Figure 1(h)–(j)].

We hypothesized that a change in NP dissolution characteristics through iron doping should lead to decreased toxicity that could be assessed through HCS. Microscopic results [high resolution TEM, electron diffraction (SAED)] and X-ray diffraction (XRD) confirmed that 10% iron loadings are possible without any detectable differences in the lattice spacing. To experimentally verify this, HRTEM image of pure ZnO with hexagonal arrangement of the lattices was structurally matched [Figure 1(a), (b)] with the crystal structure of ZnO and Fe doped ZnO. The perpendicular rows with respective *d*-spacing of 2.47(± 0.008) Å reasonably agree with $d_{011} = 2.476$ Å from XRD for both ZnO and Fe doped ZnO. A structure plot created for ZnO and Fe doped ZnO in a projection along (011) direction superimposed to high-resolution image of ZnO shows that the heavy atoms (oxygen atoms are omitted for clarity) of both structures reasonably match suggesting no detectable variations. Results from energy filtered TEM (EFTEM) show Fe is homogeneously distributed in the ZnO lattice. The dissolution of ZnO or Fe doped ZnO in aqueous solution performed in electrolyte solution was studied by adding 0.1 M NaClO₄ at pH 7 (± 0.04) and 22°C. The reaction $[\text{ZnO}_{(s)} + 2\text{H}^+ \rightarrow \text{Zn}^{2+}_{(aq)} + \text{H}_2\text{O}_{(l)}]$ was followed by periodic sampling of aliquots for total [Zn] analysis using inductively coupled plasma mass spectrometry (ICP-MS). The results show that the concentration of Zn²⁺ released by the undoped NPs rapidly exceeds the saturation of Zn²⁺ for bulk ZnO (the bulk solubility product $K_{sp} = 11.2$ implies $[\text{Zn}]^{\text{eq}} = 1.58$ mM). The Zn²⁺ release is reduced through Fe incorporation into the crystal lattice of ZnO. The inner-shell Fe-*L* edge at 708 eV gives rise to an intense fine transition responsible for overlapping of the electron cloud from the neighbouring atoms for interatomic bonding. The relatively strong σ -bonding of Fe in the host lattice of ZnO significantly reduces ZnO nanoparticle dissolution.

Electronic properties and dissolution of ZnO NPs based toxicity

The reduced dissolution of ZnO NPs is explained through the electronic properties of the engineered NPs. The results of a first-principles calculations show that Fe is substituted in Zn position.²⁰ The formation energy of Fe in ZnO suggests substitutional doping is strongly favourable for +2 oxidation state. The double Fe²⁺ substitution is more stable ($2\text{Fe}_{\text{subs}} = -1.14$ eV) compared with the single Fe²⁺ substitution ($1\text{Fe}_{\text{subs}} = -0.97$ eV).²⁰ The lattice geometry is changed by 0.03 Å in bond lengths and by 0.2° in bond angles after 10% Fe

doping. Since d^6 configuration (Fe^{2+}) requires strong ligand field to cause spin pairing in the tetraordinated system²¹ (high spin and low spin are assigned with the number of existing paired or unpaired electron in the e_g or t_{2g} orbitals), the low spin and completely occupied [Figure 1(c),(d)] d -electrons are observed in Zn and doped Fe respectively.²⁰ Consideration of the crystal field splitting of the Fe- $3d$ states implies that Fe^{2+} is more strongly bound with O than Zn^{2+} .

The ZnO dissolution (51% to 26% from 0% to 10% Fe doping respectively, supporting information) was found to play a key role for the induction of the cellular cytotoxicity (Figure 2a).^{18,22} The ZnO dissociation gives rise to increased [Zn] in the cell leading to mitochondrial damage followed by cell death. The cellular uptake as well as the material characteristics responsible for the oxidative stress determines the toxicological outcome (Figure 2b). The hierarchical oxidative stress model is associated with the level of inflammation experienced by the cell during NP exposure. Lower oxidative stress is associated with the induction of antioxidant enzymes. At higher levels of oxidative stress, the cell experience inflammation and cytotoxicity. Inflammation is initiated through the activation of pro-inflammatory signalling cascades such as mitogen-activated protein kinase (MAPK) and nuclear factor κB (NF- κB). The cell death could result from mitochondrial perturbation and the release of proapoptotic factors. The results show Zn^{2+} release are associated with ROS production and the oxidative stress pathways including intracellular calcium flux, mitochondrial depolarization, and plasma membrane leakage. After successful demonstration of the NPs dissolution induced intracellular toxicity, the engineering of ZnO NP by iron doping lead to significant reduction in toxicity proportional to the level of doping (Figure 2c).¹² Furthermore, these engineered NPs were also tested with higher organisms such as rodent and zebra fish models to conclusively establish reduced toxic effects *in vivo*.¹⁹ The toxicity in the zebra fish was evaluated in terms of embryo hatching, mortality rates and the generation of morphological defects.¹⁹ Fe-doping interfered in the inhibitory effects of Zn^{2+} on a zebra fish hatching enzyme (due to chelating property of Zn^{2+}). The toxicity assessment in the rodent lung included inflammatory cell infiltrates, lactate dehydrogenase (LDH) release and cytokine levels. The interference of inhibitory effects of Zn^{2+} by Fe doping was associated with decreased PMN cell counts, MCP-1 production, and increase in albumin levels in the mouse and rats.¹⁹

The results of the NPs toxicity in the *in vivo* sea urchin²³ showed that Fe-doped ZnO was less soluble than pure ZnO NPs. However, in contrast to the reduced toxicity observed in the *in vitro* cell culture system, no significant difference between toxicity with Fe-doped ZnO and the pure ZnO NPs was observed. The results show that the toxicity of the engineered NPs vary from organism-to-organism and from medium-to-medium. Despite reduced solubility and higher aggregation rates of Fe-doped ZnO NPs in seawater at environmentally relevant concentrations, the morphological abnormalities in developing sea urchin embryos was induced.²⁴ The toxicity is also mediated through Zn^{2+} dissolution like in the mammalian cell lines. The results highlight the importance of toxicity assessments both *in vitro* and *in vivo*, in numerous species and environmental media.

The exposure of ZnO NPs in different cell lines induce oxidative stress (through Zn^{2+} dissolution) leading to lipid peroxidation, membrane leakage, disruption of Ca^{2+}

homeostasis and ultimately cellular apoptosis.^{12,18,19} *In vivo* studies in different organisms support oxidative stress due to ZnO NPs exposure.²⁵ Poynton *et al.* reported²⁶ that different gene expression profiles observed for ZnO NP suspensions and ZnSO₄ solutions point towards ZnO dissolution induced toxicity in *D. magna*. However, other studies found that antioxidant response genes were not induced after ZnO NP exposure. Huang *et al.* reported only few antioxidant genes responding to ZnO NP in human lung epithelial cells.²⁷ In another report, although ZnO NP exposure resulted in increased reactive oxygen species (ROS), zebrafish embryos failed to initiate an antioxidant response. They inferred that the cell does not recognize ZnO NPs as Zn²⁺ and therefore does not mobilize a response comparable to Zn²⁺ treatments.²⁵ However, once inside the cell the NPs were capable of generating ROS and causing increased toxicity. In any case, the results suggest the need to make in-depth studies on the mechanism of the dissolution and the cellular outcome. To investigate this in more details, degradation of the Fe-S containing proteins might be considered as a model example for the toxicity induction since Zn²⁺ is a metal ion which can easily chelate many bioligands in the cell containing Fe-S clusters.

The Zn²⁺ interaction with Fe-S redox clusters

Extensive investigation on different mammalian cell lines showed that ZnO NPs dissolution played a major role in the toxicity generation. The reports on intracellular particle studies using *in-situ* X-ray fluorescence (μ XRF), X-ray absorption near edge structure (XANES) and synchrotron radiation X-ray fluorescence (SR-XRF) indicated that ZnO toxicity was caused by free or complexed Zn²⁺ within the cells, and not by reactions occurring on the surfaces of internalized solid phase NPs.²⁸ Hence, it is important to understand the effect of Zn²⁺ mobility in the cell in terms of interaction or chelation with different chemical species such as cellular proteins. A model for Zn²⁺ mobility and the possible cellular reactions with the Fe-S protein cluster are presented in Figure 3. Though Fe-S clusters can be chemically reconstituted, virtually all organisms contain a highly conserved, complex assembly and transfer system that facilitates the biogenesis of Fe-S cluster containing proteins.^{29,30,31} The rhombic [2Fe-2S], cuboidal [3Fe-4S], and cubane [4Fe-4S] clusters interacting with Zn²⁺ (due to ZnO NPs dissolution and effective binding with the cell organelles, supporting information) leads to altered cellular responses in the cells.³² Other common oxides such as silica and copper oxide exhibit similar behavior at elevated levels.^{33,34}

In addition, when the ZnO NP is exposed to the cell, (1) the Zn²⁺ directly opens permeability transition (PT) pores, leading to depolarization, mitochondrial swelling and cytochrome C release. Mitochondrial dysfunction (depletion of ATP) also leads to increase in ROS.³⁵ (2) The [4Fe-4S]²⁺, one of the Fe-S clusters in the family of acotinase protein are highly sensitive to oxidation and are damaged by ROS.³⁶ The oxidation of [4Fe-4S]²⁺ by ROS produces an intermediate product [4Fe-4S]²⁺. OO²⁻ which reacts with available proton giving [4Fe-4S]³⁺. The [4Fe-4S]³⁺ cluster releases³⁷ Fe²⁺ giving rise to hierarchical OS¹¹ eventually producing inactive [3Fe-4S]⁰ after univalent reduction of [3Fe-4S]³⁺.³⁸ (3) *In vitro* studies have also revealed that Zn²⁺ not only reacts with previously assembled iron-sulphur clusters, but also with the unstable iron-sulphur clusters during biosynthesis.³⁹ The cellular properties with respect to decrease in the iron counts are due to the combination of Zn²⁺ with Fe-S cluster to give ZnFe₃S₄ (a product⁴⁰ from the reaction of Zn²⁺ and degraded

cluster). (4) Regeneration of the active $[4\text{Fe-4S}]^{2+}$ in the cell is efficiently achieved through the reduction of the oxidized cluster and subsequent insertion of a ferrous ion from Fe-doped ZnO (iron pool) to rectify further cytotoxicity. Our results of ZnO and Fe doped ZnO NPs on the activity of Fe-S containing proteins showed that the citrate was isomerized into isocitrate, which was converted to α -ketoglutarate in a reaction catalyzed by isocitric dehydrogenase. These reactions were monitored through measuring the increase in absorbance at 340 nm associated with the formation of NADPH where the rate was proportional to protein activity. The rate of enzyme activity was also lowered significantly after addition of ZnO compared to the increased rate of enzyme activity after addition of Fe doped ZnO. Jang *et al.* reported the electron transfer from the iron-sulfur cluster because the reaction with H_2O_2 generates unstable $[4\text{Fe-4S}]^{3+}$ moieties in *Escherichia coli*. The cluster gained stability by releasing Fe^{2+} to form inactive $[3\text{Fe-4S}]^+$. Damaged clusters were reassembled chemically with dithiothreitol and Fe^{2+} treatment, where 60% activity was regenerated within 3 min.⁴¹ The result shows a possible regeneration of the active protein moiety by the univalent reduction of the oxidized cluster and subsequent insertion of a ferrous ion from a Fe doped ZnO also in the mammalian cell lines to steer the cell into normal functioning as described in the present model (Figure 3). In summary, the mechanistic understanding of ZnO nanoparticle toxicity was addressed by flame aerosol engineered (Fe-doped) materials yielding less soluble particles that offer an improved safety margin. In-depth understanding of mechanisms of nano-bio-interactions is required to develop such safe-by-design strategy through addressing details of the cellular functions and metabolisms.

Apart from NPs dissolution induced oxidative stress, light induced phototoxicity is another oxidative stress paradigm.⁴² UV can excite electrons into the conduction band of the NPs such as TiO_2 creating an electron-hole pair.⁴² The generated charge interacts with H_2O and molecular oxygen to generate $\text{HO}\cdot$ radicals and superoxides.⁴³ However, the intrinsic toxic effects of light with high energy wavelengths responsible for the e^-/h^+ pair generation is a challenge in determining the potential phototoxicity of TiO_2 . TiO_2 is reported as a strong candidate for the biological injury even in the absence of light because the conduction band is situated almost to the same level of the oxidative stress potential $[\text{O}_2 + e^- \rightarrow \text{O}_2^- (E^\circ = -4.3 \text{ eV})]$ $E^\circ = \text{standard electrode potential}$.⁴⁴

Since FSP was versatile in engineering ZnO NPs by Fe doping, TiO_2 based NP library (undoped or Fe doped) was synthesized using flame spray pyrolysis (FSP).^{45,46} Results showed Fe loading was able to lower the band gap energy ($E_{\text{TiO}_2} = 3.2 \text{ eV}$ to

$E_{\text{Fe doped TiO}_2} = 2.8 \text{ eV}$) through introduction of trap levels between the valence and conduction bands.⁴⁵ These trap levels allow for excitation of electrons when subjected to near-visible (350–450 nm) light illumination. The results of the NPs exposed cells with near visible light showed the increase in Fe loading increased the % of cell death [Figure 4].

The independent experiments performed for the verification of the ROS generation during light irradiation in the cell [Figure 4(a)] showed (a) spontaneous degradation [Figure 4(b)] of *N*-acetyl-L-tryptophanamide (NATA) a biomolecule used for ROS capture during photochemical reactions in the cells (b) multi-parameter responses (superoxide generation, loss of mitochondrial membrane potential (MMP) and PI uptake) increased with Fe content

[Figure 4(c)] (c) cells pre-treated with N-acetyl cysteine (NAC, a free radical quencher) failed to show any ROS in the cell. This is a clear indication of the light induced ROS responsible for the bio-reaction and phototoxicity (oxidative stress) in the cell.

In summary, the radical generation from light activated NPs in the cell is responsible for the phototoxicity. The specific design using flame spray pyrolysis (FSP) appears to be instrumental for band gap tuning and the introduction of trap levels for electron capture during light exposure. With the proven ability of the FSP to obtain fine particles and the phototoxicity evaluation method, the present concept of toxicity determination can be generalized for other photoactive materials.

Future outlook for designing safer nanoparticles and the state-of-the-art of double flame FSP

In the last decade nanoscale materials have been prepared using a single flame reactor. Compared to the single flame setup, the stereoscopic two-flame reactor has further advantages such as flexibility for the control of important flame parameters affecting particle formation, and affording the control of particle mixing at the nano-level in multicomponent systems. In the double flame approach, the particles are designed in two independent flames before the nanoparticles are collected (see Figure 5). The manipulation of the nozzle distance, the flame angles and the defined distance at which two particle streams intersect give rise to innumerable possibilities for engineering nanoparticles for different applications. The double flame approach was first used by Strobel *et al.* to synthesize Pt loaded Ba/Al₂O₃ multicomponent catalyst for NO_x storage.⁴⁷⁻⁴⁹ Minnermann *et al.* used two individual flames in tuning the alumina and cobalt oxide Fischer-Tropsch catalysts.⁵⁰ The individual components were individually controlled in each flame with respect to composition and size through adjusting the intersection distance of the flame. Such investigations on the influence of the intersection distances are rare in designing nanoparticles for different applications. The thermodynamically favourable inactive spinels such as CoAl₂O₄, FeAl₂O₄, Fe₂SiO₄, Co₂SiO₄ that are not reduced at the catalysts operating temperatures are major phases produced during the material synthesis. These spinels were efficiently avoided by tuning the flame angles and the particle stream intersection distances.⁵⁰ Moreover, the double flame reactor also enables the homogeneous active metal dispersion with control over particle size and chemical aggregation. In another example, FSP was utilized for the preparation of Pd-silica/alumina system for tuning Brønsted acid sites on the surface of the nanoparticles. The density of the Brønsted acid sites could be tuned with the incorporation of the differing aluminium content in the vicinity of a silanol group.⁵¹ These inherent acid sites could be tailored for varying pH of the cellular medium during toxicity testing. Recent developments based on molecular and/or nanostructure designs have led to advances towards light-induced charge separation and subsequent catalytic water oxidation and reduction reactions.⁵² Developing nanoscale material, that focus on the development of visible-light active hetero-nanostructures is possible using double flame setup. If more than one type of nanoparticle is interacting in the environment, there can be protecting effects against ROS reduction or there might be metal ion adsorption or even incorporation into the second nanoparticle. However, there can also be more severe effects introduced by electron transfer between the NP and the intermediate reactions

(antenna effect). This can be effectively studied using versatile double flame system for efficient *in-situ* mixing of the nanoparticles at the nano-level forming heterojunction for effective charge transfer.

Conclusion

The rapid multi-parametric screening assessment shows that the ZnO and TiO₂ are toxic due to particle dissolution and shedding of toxic Zn²⁺ and e⁻h⁺ pair generation after irradiating with visible light, respectively. ZnO toxicity is reduced through Fe-doping which leads to a stabilization of crystal structure. In contrast, Fe doping increases the photo-toxicity. Overall, our study demonstrates the utility of integrated cytotoxicity screening assays to assess nanomaterial hazard as well as to improve material safety through rational modification. The Fe which is doped in both the NPs (TiO₂ and ZnO) using versatile FSP system changed the material property with respect to toxicity. From the results obtained for ZnO and TiO₂, it is clear that nanoscale materials need to be engineered to harvest intrinsic properties. The innovation in designing new particles lies in manipulating the reactor systems where the reaction parameters can be effectively controlled. Compared to the single flame setup, the two-flame reactor has innumerable advantages such as control over flame parameters, homogeneous multicomponent mixing, and control over nozzle distances (designing the intersection point of the two independent particle stream) and flame angle. To effectively design nanoparticles, a future outlook for and the state of the art of the double flame FSP is described.

Supplementary Material

Refer to Web version on PubMed Central for supplementary material.

Acknowledgments

This material is based upon the work supported by the National Science Foundation and the Environmental Protection Agency under Cooperative Agreement Number DBI-0830117. Any opinions, findings, and conclusions or recommendations expressed in this material are those of the author(s) and do not necessarily reflect the views of the National Science Foundation or the Environmental Protection Agency. This work has not been subjected to EPA review and no official endorsement should be inferred. Key support was provided by the US Public Health Service Grants U19 ES019528 (UCLA Center for NanoBiology and Predictive Toxicology), RO1 ES016746, and RC2 ES018766. We thank Prof. J. I. Zink, Dr. T. Xia and Dr. S. George, CEIN, UCLA, for the useful discussion. We also thank Prof. A. Rosenauer and Dr. M. Schowalter, Department of Physics for Microscopic measurements. We are thankful to Dr. J. Birkenstock, Department of Geology, University of Bremen and Dr. H. J. Zhang, IWT, Foundation Institute of Material science, University of Bremen for discussion.

References

1. Joner, E.J.; Hartnik, T.; Amundsen, C.E. Nanoparticles and the environment (TA-2304/2007). *Bioforsk, Ås*; 2007. p. 1-64.
2. Xia Y. Nanomaterials at work in biomedical research. *Nat Mater*. 2008; 7(10):758–760. [PubMed: 18813296]
3. Buzea C, Pacheco II, Robbie K. Nanomaterials and nanoparticles: Sources and toxicity. *Biointerphases*. 2007; 2(4):MR17–MR71. [PubMed: 20419892]
4. Niederberger M. Nonaqueous Sol-gel routes to metal oxide nanoparticles. *Acc Chem Res*. 2007; 40(9):793–800. [PubMed: 17461544]

5. Pokhrel S, Simion CE, Teodorescu VS, Barsan N, Weimar U. Synthesis, mechanism, and gas-sensing application of surfactant tailored tungsten oxide nanostructures. *Adv Funct Mater.* 2009; 19(11):1767–1774.
6. Teoh WY, Amal R, Mädler L. Flame spray pyrolysis: an enabling technology for nanoparticles design and fabrication. *Nanoscale.* 2010; 2(8):1324–1347. [PubMed: 20820719]
7. Pokhrel S, Birkenstock J, Schowalter M, Rosenauer A, Mädler L. Growth of ultrafine single crystalline WO₃ nanoparticles using flame spray pyrolysis. *Crystal Growth & Design.* 2010; 10(2): 632–639.
8. Kemmler JA, Pokhrel S, Birkenstock J, Schowalter M, Rosenauer A, Nicolae Bârsan N, Udo Weimar U, Mädler L. Quenched, nanocrystalline In₄Sn₃O₁₂ high temperature phase for gas sensing applications. *Sens and Actuators B.* 2012; 161(1):740–747.
9. Nel AE, Mädler L, Velegol D, Xia T, Hoek EMV, Somasundaran P, Klaessig F, Castranova V, Thompson M. Understanding biophysicochemical interactions at the nano-bio interface. *Nat Mater.* 2009; 8(7):543–557. [PubMed: 19525947]
10. Hussain SM, Braydich-Stolle LK, Schrand AM, Murdock RC, Yu KO, Mattie DM, Schlager JJ, Terrones M. Toxicity evaluation for safe use of nanomaterials: recent achievements and technical challenges. *Adv Mater.* 2009; 21(16):1549–1559.
11. Nel A, Xia T, Mädler L, Li N. Toxic potential of materials at the nanolevel. *Science.* 2006; 311(5761):622–627. [PubMed: 16456071]
12. George S, Pokhrel S, Xia T, Gilbert B, Ji ZX, Schowalter M, Rosenauer A, Damoiseaux R, Bradley KA, Mädler L, Nel AE. Use of a rapid cytotoxicity screening approach to engineer a safer zinc oxide nanoparticle through iron doping. *ACS Nano.* 2010; 4(1):15–29. [PubMed: 20043640]
13. Dürr O, Duval F, Nichols A, Lang P, Brodte A, Heyse S, Besson D. Robust hit identification by quality assurance and multivariate data analysis of a high-content, cell-based assay. *J Biomol Scr.* 2008; 12(8):1042–1049.
14. Dahl JA, Maddux BLS, Hutchison JE. Toward greener nanosynthesis. *Chem Rev.* 2007; 107(6): 2228–2269. [PubMed: 17564480]
15. Mädler L, Stark WJ, Pratsinis SE. Rapid synthesis of stable ZnO quantum dots. *J Appl Phys.* 2002; 92(11):6537–6540.
16. Mueller R, Mädler L, Pratsinis SE. Nanoparticle synthesis at high production rates by flame spray pyrolysis. *Chem Eng Sci.* 2003; 58(10):1969–1976.
17. Wegner K, Pratsinis SE. Flame synthesis of nanoparticles. *Chem Today.* 2004; 22(6):27–29.
18. Xia T, Kovoichich M, Liang M, Mädler L, Gilbert B, Shi H, Yeh JI, Zink JI, Nel AE. Comparison of the mechanism of toxicity of zinc oxide and cerium oxide nanoparticles based on dissolution and oxidative stress properties. *ACS Nano.* 2008; 2(10):2121–2134. [PubMed: 19206459]
19. Xia T, Zhao Y, Sager T, George S, Pokhrel S, Li N, Schoenfeld D, Meng H, Lin S, Wang X, Wang M, Ji Z, Zink JI, Mädler L, Castranova V, Lin S, Nel AE. Decreased dissolution of ZnO by iron doping yields nanoparticles with reduced toxicity in the rodent lung and zebrafish embryos. *ACS Nano.* 2011; 5(2):1223–1235. [PubMed: 21250651]
20. Xiao J, Kuc A, Pokhrel S, Schowalter M, Parlapalli S, Rosenauer A, Frauenheim T, Mädler L, Petterson LGM, Heine T. Evidence for Fe²⁺ in wurtzite coordination: iron doping stabilizes ZnO nanoparticles. *Small.* 2011; 7(20):2879–2886. [PubMed: 21913325]
21. Cotton, FA.; Wilkinson, G.; Murrillo, CA.; Bochmann, M. *Advanced Inorganic Chemistry.* 6. John Wiley & Sons, Inc; 1999. p. 776-814.
22. Damoiseaux R, George S, Li M, Pokhrel S, Ji Z, France B, Xia T, Suarez E, Rallo R, Madler L, Cohen Y, Hoek EMV, Nel A. No time to lose-high throughput screening to assess nanomaterial safety. *Nanoscale.* 2011; 3(4):1345–1360. [PubMed: 21301704]
23. Fairbairn EA, Keller AA, Mädler L, Zhou D, Pokhrel S, Cherr GN. Metal oxide nanomaterials in seawater: Linking physicochemical characteristics with biological response in sea urchin development. *J Hazard Mater.* 2011; 192(3):1565–1571. [PubMed: 21775060]
24. Li M, Pokhrel S, Jin X, Mädler L, Damoiseaux R, Hoek EMV. Stability, bioavailability, and bacterial Toxicity of ZnO and iron-doped ZnO nanoparticles in aquatic media. *Env Sci & Technol.* 2011; 45(2):755–761. [PubMed: 21133426]

25. Wong S, Leung P, Djurišić A, Leung K. Toxicities of nano zinc oxide to five marine organisms: influences of aggregate size and ion solubility. *Anal Bioanal Chem.* 2010; 396(2):609–618. [PubMed: 19902187]
26. Poynton HC, Lazorchak JM, Impellitteri CA, Smith ME, Rogers K, Patra M, Hammer KA, Allen HJ, Vulpe CD. Differential gene expression in daphnia magna suggests distinct modes of action and bioavailability for ZnO nanoparticles and Zn ions. *Env Sci & Technol.* 2011; 45(2):762–768. [PubMed: 21142172]
27. Huang CC, Aronstam RS, Chen DR, Huang YW. Oxidative stress, calcium homeostasis and altered gene expression in human lung epithelial cells exposed to ZnO nanoparticles. *Toxicol in Vitro.* 2010; 24(1):45–55. [PubMed: 19755143]
28. Gilbert B, Fakra SC, Xia T, Pokhrel S, Mädler L, Nel AE. The Fate of ZnO nanoparticles administered to human bronchial epithelial cells. *ACS Nano.* 2012; 6(6):4921–4930. [PubMed: 22646753]
29. Mansy SS, Cowan JA. Iron-sulfur cluster biosynthesis: toward an understanding of cellular machinery and molecular mechanism. *Acc Chem Res.* 2004; 37(9):719–725. [PubMed: 15379587]
30. Holm RH. Synthetic approaches to the active sites of iron-sulfur proteins. *Acc Chem Res.* 1977; 10(12):427–434.
31. Seefeldt LC, Dean DR. Role of nucleotides in nitrogenase catalysis. *Acc Chem Res.* 1997; 30(6):260–266.
32. Volbeda A, Charon MH, Piras C, Hatchikian EC, Frey M, Fontecilla-Camps JC. Crystal structure of the nickel-iron hydrogenase from *Desulfovibrio gigas*. *Nature.* 1995; 373(6515):580–587. [PubMed: 7854413]
33. Brunner TJ, Wick P, Manser P, Spohn P, Grass RN, Limbach LK, Bruinink A, Stark WJ. In vitro cytotoxicity of oxide nanoparticles: comparison to asbestos, silica, and the effect of particle solubility. *Env Sci & Technol.* 2006; 40(14):4374–4381. [PubMed: 16903273]
34. Studer AM, Limbach LK, Van Duc L, Krumeich F, Athanassiou EK, Gerber LC, Moch H, Stark WJ. Nanoparticle cytotoxicity depends on intracellular solubility: comparison of stabilized copper metal and degradable copper oxide nanoparticles. *Toxicol Lett.* 2010; 197(3):169–174. [PubMed: 20621582]
35. Gazaryan IG, Krasinskaya IP, Kristal BS, Brown AM. Zinc irreversibly damages major enzymes of energy production and antioxidant defense prior to mitochondrial permeability transition. *J Bio Chem.* 2007; 282(33):24373–24380. [PubMed: 17565998]
36. Flint DH, Tuminello JF, Emptage MH. The inactivation of iron-sulphur cluster containing hydrolyases by superoxide. *J Biol Chem.* 1993; 268(30):22369–76. [PubMed: 8226748]
37. Leal SNS, Gomes CUM. Linear three-iron centres are unlikely cluster degradation intermediates during unfolding of iron-sulfur proteins. *Biol Chem.* 2005; 386(12):1295–1300. [PubMed: 16336124]
38. Gardner PR, Raineri Is, Epstein LB, White CW. Superoxide radical and iron modulate aconitase activity in mammalian cells. *J Biol Chem.* 1995; 270(22):13399–13405. [PubMed: 7768942]
39. Iwasaki T. Iron-sulfur world in aerobic and hyperthermoacidophilic archaea *Sulfolobus*. *Archaea.* 2010; 2010:Article ID 842639, 14.
40. Srivastava KKP, Surerus KK, Conover RC, Johnson MK, Park JB, Adams MWW, Munck E. Mössbauer study of zinc-iron-sulfur $ZnFe_3S_4$ and nickel-iron-sulfur $NiFe_3S_4$ clusters in *Pyrococcus furiosus* ferredoxin. *Inorg Chem.* 1993; 32(6):927–936.
41. Jang S, Imlay JA. Micromolar intracellular hydrogen peroxide disrupts metabolism by damaging iron-sulfur enzymes. *J Biol Chem.* 2007; 282(2):929–937. [PubMed: 17102132]
42. Hoffmann MR, Martin ST, Choi W, Bahnemann DW. Environmental applications of semiconductor photocatalysis. *Chem Rev.* 1995; 95(1):69–96.
43. Sinha RP, Hader DP. UV-induced DNA damage and repair: a review. *Photochem Photobiol Sci.* 2002; 1(4):225–236. [PubMed: 12661961]
44. Burello E, Worth PA. A theoretical framework for predicting the oxidative stress potential of oxide nanoparticles. *Nanotoxicology.* 2010; 5(2):228–235. [PubMed: 21609138]

45. George S, Pokhrel S, Ji Z, Henderson BL, Xia T, Li L, Zink JI, Nel AE, Mädler L. Role of Fe doping in tuning the band gap of TiO₂ for the photo-oxidation induced cytotoxicity paradigm. *J Am Chem Soc.* 2011; 133(29):11270–11278. [PubMed: 21678906]
46. Teoh WY, Amal R, Mädler L, Pratsinis SE. Flame sprayed visible light-active Fe-TiO₂ for photomineralisation of oxalic acid. *Catal Today.* 2007; 120 (2):203–213.
47. Strobel R, Krumeich F, Pratsinis SE, Baiker A. Flame-derived Pt/Ba/Ce_xZr_{1-x}O₂: Influence of support on thermal deterioration and behavior as NO_x storage-reduction catalysts. *J Catal.* 2006; 243(2):229–238.
48. Strobel R, Mädler L, Piacentini M, Maciejewski M, Baiker A, Pratsinis SE. Two-nozzle flame synthesis of Pt/Ba/Al₂O₃ for NO_x storage. *Chem Mater.* 2006; 18 (10):2532–2537.
49. Strobel R, Pratsinis SE. Flame aerosol synthesis of smart nanostructured materials. *J Mater Chem.* 2007; 17(45):4743–4756.
50. Minnermann M, Großmann H, Pokhrel S, Thiel K, Hagelin-Weaverd H, Bäumer M, Mädler L. Double flame spray pyrolysis as a novel technique to synthesize alumina-supported cobalt Fischer-Tropsch catalysts. *Catal Today.* 2012 Manuscript submitted.
51. Huang J, van Vegten N, Jiang Y, Hunger M, Baiker A. Increasing the Brønsted acidity of flame-derived silica/alumina up to zeolitic strength. *Angew Chem Int Ed.* 2010; 49 (42):7776–7781.
52. Tachibana Y, Vayssieres L, Durrant JR. Artificial photosynthesis for solar water-splitting. *Nat Photon.* 2012; 6:511–518.

Biographies

Suman Pokhrel received his PhD with JNU Fellowship in 2005 from the Madras University, India. He joined School of Chemistry and Materials Science, Heilongjiang University, China for his postdoctoral work in the year 2005–2006. He was awarded a Georg Forster Fellow of AvH Foundation in the Tübingen University, Germany in 2006. Presently he is working as a Research scientist in the Foundation Institute of Materials Science in the group of Prof. Lutz Mädler, University of Bremen. His research interests include synthesizing oxide nano-structured materials for various applications using soft chemistry routes and Flame Spray Pyrolysis (FSP).

André E. Nel, Professor of Medicine and Chief, Division of NanoMedicine at UCLA, directs the University of California Center for the Environmental Impact of Nanomaterials and UCLA center for Nanobiology and Predictive Toxicology. He obtained his MD and doctorate degrees from Stellenbosch University in Cape Town, South Africa. His chief research interests are nano EHS, nanobiology and nanotherapeutics.

Lutz Mädler received his Ph.D. from Univ. Freiberg/Sa., Germany in 1999 and received his Habilitation in 2003 at Swiss Federal Institute of Technology (ETH Zurich). He was Senior Lecturer at the Department of Chemical Engineering, University of California, before he joined the Department of Production Engineering at the University of Bremen leading the Particle and Process Technology division in 2008. He is also Director at the Foundation Institute of Materials Science. His research focuses on integrated aerosol processes for nanomaterials and surface films for sensors, catalysts, and optical devices, and on nano-bio-interactions.

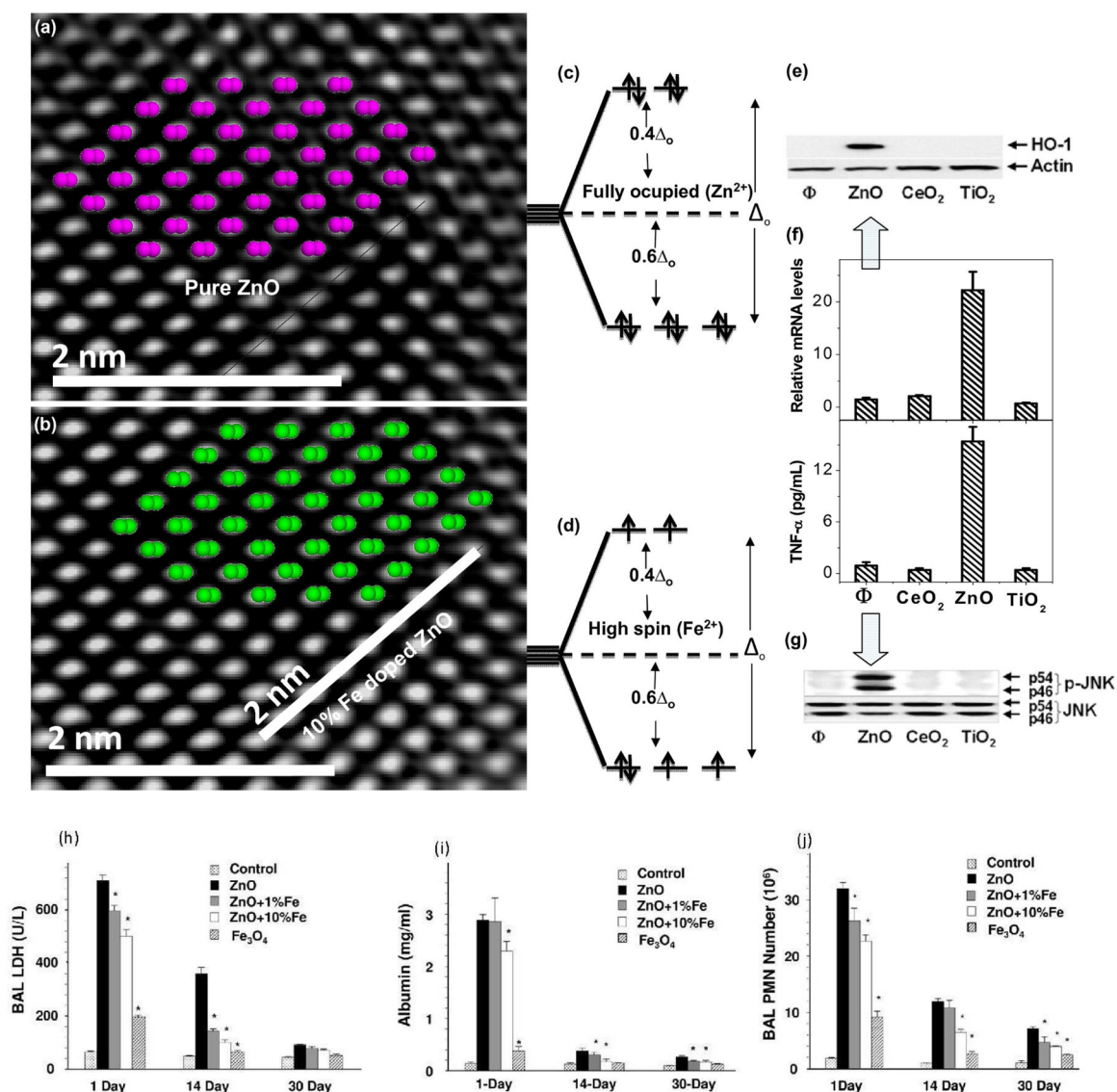


Figure 1.

Physicochemical characterization of undoped and Fe doped ZnO NPs. [(a),(b) Matching crystal structure with HRTEM image for undoped and Fe doped ZnO. No detectable structural deviation observed [(c),(d) d -orbitals splitting of Zn^{2+} and Fe^{2+} [(e)–(g)] Induction of HO-1 expression and Jun kinase activation by immuno-blotting and TNF- α activation of ZnO, CeO_2 or TiO_2 (h)–(j) Time dependent toxicity evaluation. Animals were euthanized and BAL fluid was collected to determine PMN numbers, LDH, and albumin levels (supplementary section).^{18,19}

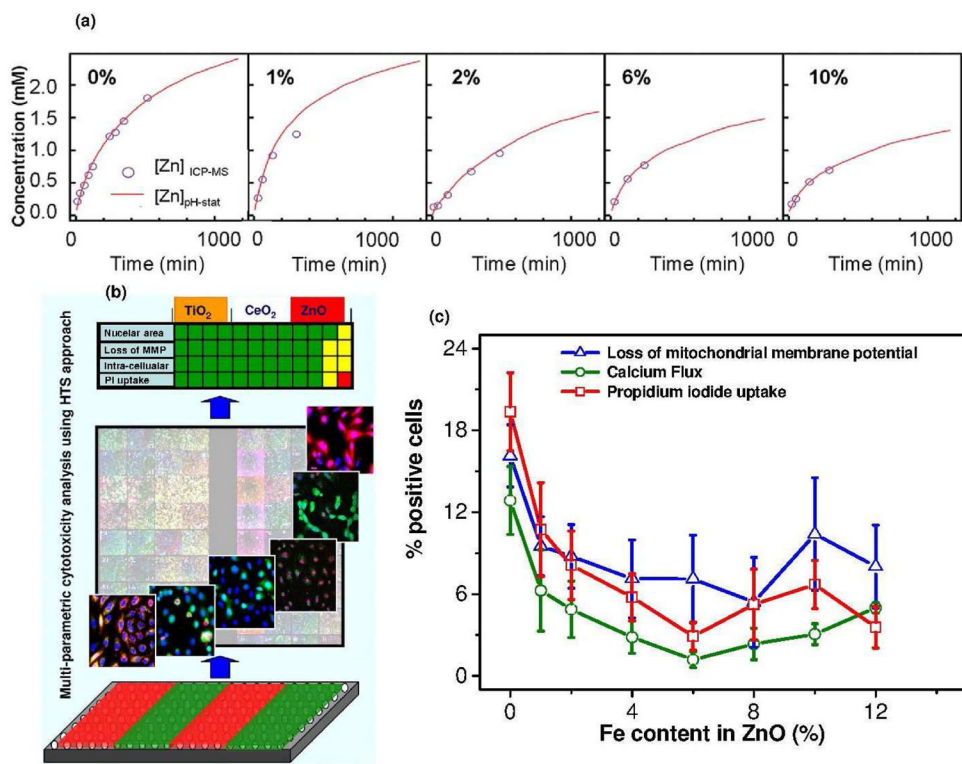


Figure 2. (a) Dissolution kinetics of pure or Fe doped ZnO NPs (b) Toxicity evaluation for ZnO, CeO₂ or TiO₂ with florescent dyes (c) toxicity reduction with increase in Fe content in ZnO (safe-by-design strategy).¹²

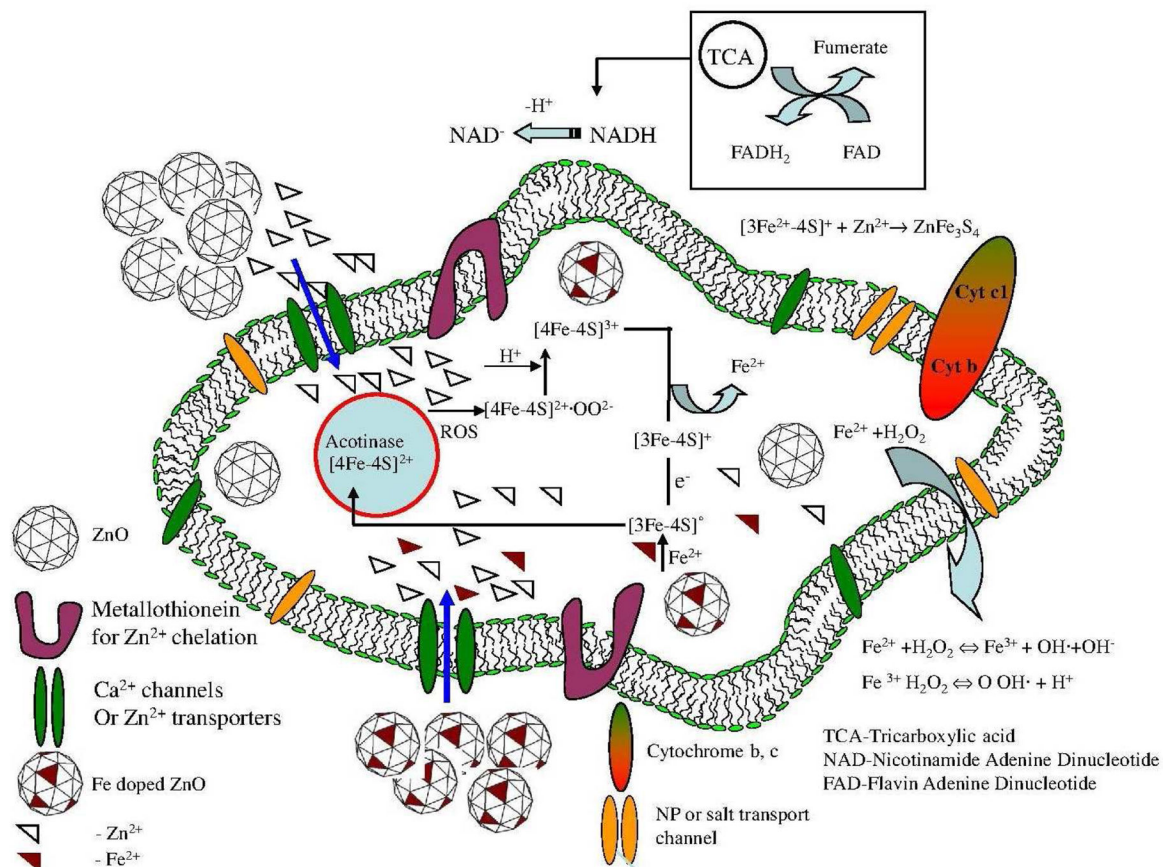


Figure 3. The Fe-S cluster degradation and respective charge transfer during the cellular Fe-S cluster metabolism through ZnO exposure and rectification of the protein with subsequent Fe addition through doped ZnO NPs. The channels in the cell membranes enhance the ions to migrate inside the cell for complex reactions as shown in the figure.

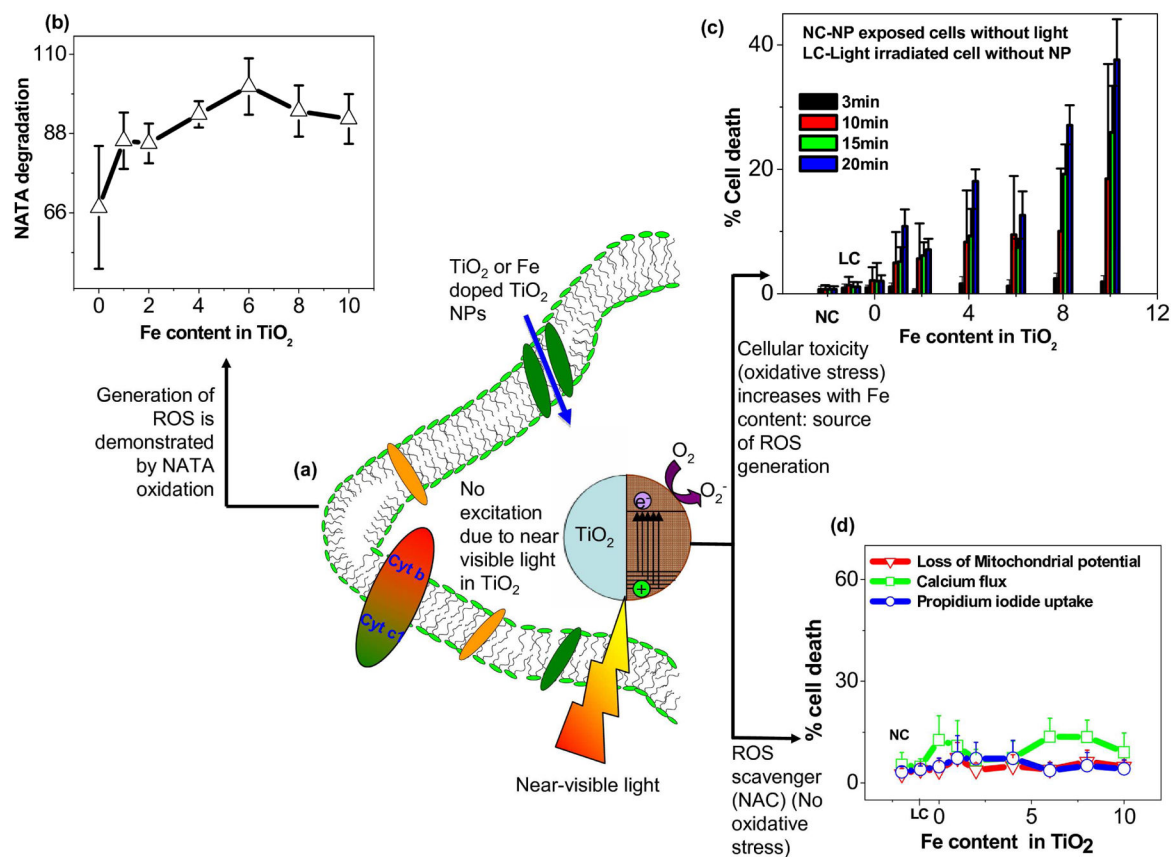


Figure 4.

Near-visible light induced ROS and evidence of the oxidative stress (a) near-visible light irradiation of TiO₂ or Fe doped TiO₂ NPs in the cell, (b) ROS causing NATA degradation in the cell, (c) High throughput screening (HTS) used to determine cell death accompanied by various oxidative stress pathways, (d) oxidative stress scavenger (NAC) for demonstrating the reduction of the phototoxicity.⁴⁵

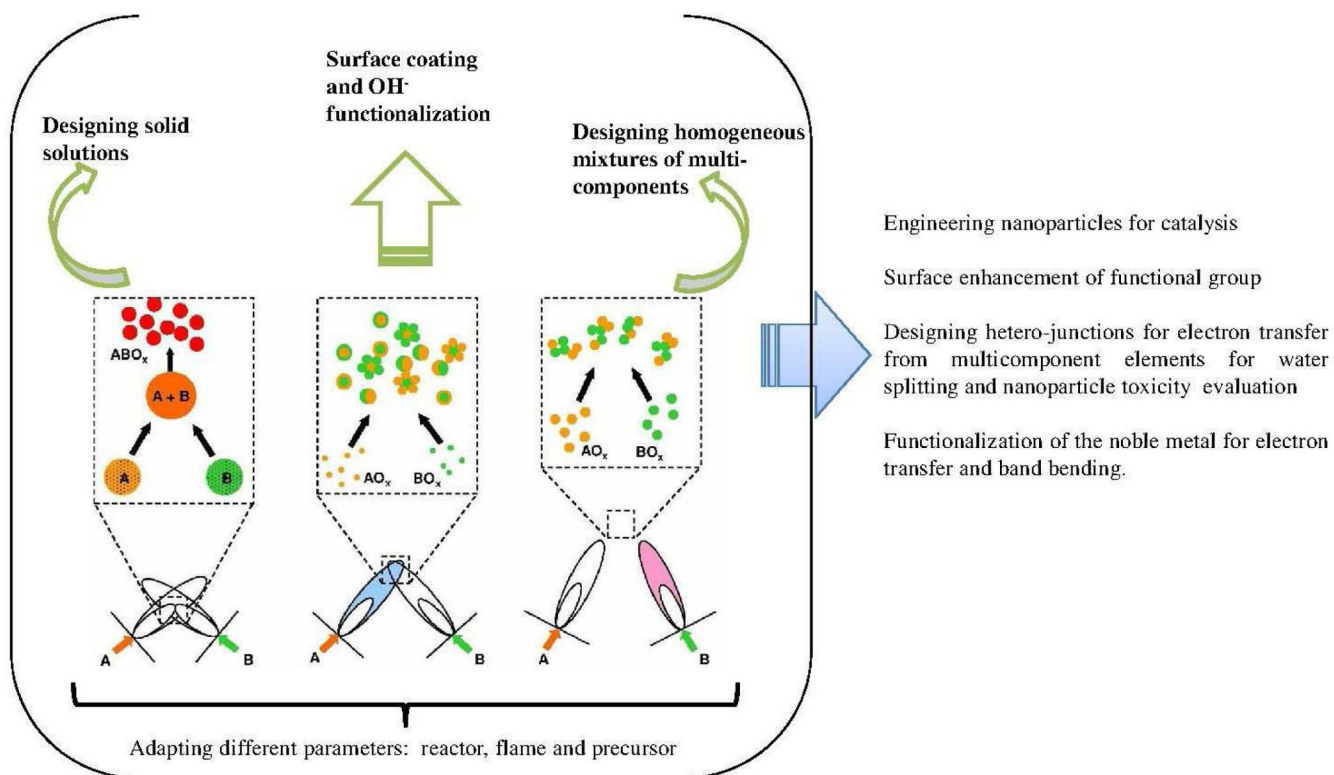


Figure 5. The versatile two reactor systems and the flame symmetry of flame spray pyrolysis for designing next generation nanoscale materials.